SUPPLEMENTAL METHODS

Quantitative Real-Time Polymerase Chain Reaction.

Total RNA extracted from different tissues with the Micro-to-Midi Total RNA Purification System (Invitrogen Life Technologies, Carlsbad, CA, USA) was used for cDNA preparation by reverse transcription with Superscript II Reverse Transcriptase and random primers (Invitrogen). For qPCR (Supplemental Fig. 1), a TaqMan® Gene expression Assay from Applied Biosystems (Foster City, CA, USA) was used in an ABI Prism 7000. Expression levels of CRIg were normalized for glyceraldehydes-3-phosphate dehydrogenase levels by the $2^{-\Delta\Delta CT}$ method (*1*).

CRIg Recombinant Protein Production.

Recombinant mouse CRIg-Hexahistidine (His) tagged protein was generated by transformation of a modified pES31 expression vector (*2*) containing the extracellular domains of mouse CRIg into HEK293T cells. The protein was purified over a nickel column followed by a Sephacryl S-200 gel filtration (VIB protein facility, Gent, BE). Protein purity was evaluated by Coomassie-stained SDS-PAGE gels. Protein concentrations were determined spectrophotometrically at 280 nm.

Nanobody Generation and Purification.

Nbs were produced as described previously (*3*). In brief, a Nb phage library with an estimated 7.27×10^7 clones was generated by using peripheral blood lymphocytes isolated from an alpaca (*Vicugna pacos*) immunized with recombinant mouse CRIg protein. After three rounds of selection against recombinant mouse CRIg, Nbs were isolated and tested for CRIg specificity in an ELISA using recombinant mouse CRIg. The distinct clones were subcloned into the pHEN6 expression vector (*4*) which fuses a 6xHis tag to the Nb C-terminus. For immunofluorescence microscopy, the CRIg-specific NbV4m119 were subcloned into the pMECS vector which

inserted a hemaglutinin (HA) tag in between the VHH and His tag. All Nbs were produced in the periplasm of *Escherichia coli* WK6 cells as described previously (*5*).

Surface Plasmon Resonance (SPR).

Nb affinity was determined using SPR (Biacore T200, GE Health) by passing different 1 nM – 400 nM concentrations over 400 RU of recombinant mouse CRIg protein coupled to a CM5 chip. Affinity constants were calculated using a 1:1 binding model in the BIAevaluation T200 software (GE Healthcare).

CRIg Transfectants.

CHO cells expressing the membrane bound form of mouse CRIg were generated by lipofection of a modified pES31 expression vector containing the full-length mouse CRIg gene and a neomycin resistance cassette. Clones were selected using flow cytometry with an anti-CRIg monoclonal antibody which was generously provided by Genentech. Both this and the corresponding isotype control antibody (R&D) were labeled by lightning-link APC conjugation kit (Innova biosciences).

Liver Cell Preparation and Cytofluorometry Analysis.

Liver single-cell suspensions were obtained by digesting liver homogenate in HBSS containing collagenase III for 30 min at 37°C, and passed through a 0.7-micron cell strainer. Erythrocytes were lysed in erythrocyte lysis buffer pH 7.2, following three centrifugation steps of 600g for 10min at 4°C to remove the hepatocytes. Anti-CD45.2 (Cl:104)/FITC, anti-CD11b (M1/70)/PE-Cy7, anti-F4/80(CI:BM8)/APC-eFluor780 antibodies were purchased from eBioscience. Nbs were labeled using the Alexafluor647 protein labeling Kit (Invitrogen) according to the manufacturers' instructions. 0.5ug of antibody and Nb were used per million cells. Flow

cytometry analyses were performed on a FACS Canto II and histograms were prepared using FlowJo software (Becton Dickinson, San Jose, CA).

^{99m}Tc-Nanobody Labeling and Pinhole SPECT/μCT Analysis.

Nbs were labeled with ^{99m}Tc via their his tag as described before (*3*, *6*). ^{99m}Tc-labeling efficiency was determined by instant thin-layer chromatography in acetone as mobile phase. The ^{99m}Tc-Nb solution was purified on a NAP-5 column (GE Healthcare) and then passed through a Millex-GV4 0.22-mm filter (Millipore). C57BL/6J mice or DBA/1 mice were injected intravenously with 80-100μl of 99mTc- Nbs. 1.427 ± 0.5306 mCi (90 mice ± SEM) of 99mTc- Nbs activity was injected per mouse. At 1h (naive mice) or 3h (CIA mice) post injection, anesthetized mice were imaged using μCT (Skyscan 1178; Skyscan) followed by pinhole SPECT (e.cam180; Siemens Medical Solutions) as described previously (*7*). ^{99m}Tc-NbV4m119 accumulation in specific inflamed regions was quantified as %IA normalized for the region of interest size. 20-30 min after SPECT/CT imaging, mice were sacrificed, tissues were dissected and weighed, and their radioactivity content was measured using an automated γ-counter (Cobra II Inspector 5003; Canberra-Packard, Schwadorf, Austria). Organ uptake was calculated as the percentage of injected activity per gram (%IA/g) and corrected for decay.

Immunofluorescence Microscopy.

Inflamed knee synovia were embedded in Tissue-Tek OCT (Sakura), frozen in liquid nitrogen. Cryostat sections (5μm) were fixed in 3% paraformaldehyde (pH7.4) and incubated in 1% PBS/BR containing detection antibodies. Nb-HA tag and anti-CD68/biotin (AbD Serotec) were amplified using anti-HA/Alexafluor488 and Streptavidin-Alexafluor568 (Molecule Probes) in 1% PBS-BR, respectively. Fluoro-Gel II/DAPI (Electron Microscopy Sciences) mounted slides were used for confocal microscopy with a plan-apochromat 20x/0.80 or LD C-apochromat 30x/1.1 W

DICIII objective on a Zeiss confocal laser scanning microscope (LSM-710) and Zen 2009 software.

Anti-CRIg Nanobody Generation and Characterization.

Screening of the phage library against mCRIg yielded 3 distinct groups of Nbs, based on sequence similarity of the antigen-binding loops. After mCRIg specific ELISA screening, 9 Nbs from group 1 and 2 were selected for further analysis. All selected Nbs bound to mCRIg antigen with high affinities ranging from 0.94 to 32.3 nmol/L as determined by SPR (Supplemental Table 1, Supplemental Fig. 5). Flow cytometry analysis confirmed that these Nbs recognized CRIg expressed on CRIg transfectants (Supplemental Fig. 6). Based on these biochemical properties, Nbs NbV4m119 and NbV4m62 representing group 2 and NbV4m68 representing group 1 were selected as the three leading candidates. All three selected Nb clones were labeled with ^{99m}Technetium (^{99m}Tc), in order to determine whether the Nbs can target CRIg positive tissue in vivo. After ^{99m}Tc-radiolabeling and subsequent purification steps, radiochemical purities were 99% for all Nbs except for ^{99m}Tc-NbV4m68 (93%). In concordance with the tissue mRNA expression studies, ^{99m}Tc-anti-CRIg Nb uptake in the liver was higher for all three clones as compared to the non-targeting control ^{99m}Tc-NbBCII10 (P<0.05) (Supplemental Fig. 7).

When ^{99m}Tc labeled CRIg Nbs were compared, ^{99m}Tc-NbV4m119 had both the highest absolute accumulation in the liver (23.6±0.1%IA/g versus BCII10 0.6±0.1%IA/g) as well as the best liver to blood ratio (28.4±3.2 versus BCII10 1.2±0.1) or tissue ratios (116.3±17.5 versus BCII10 4.7±1.5) (Supplemental Table 2). Because NbV4m119 also had the best affinity in SPR (0.9 nmol/l), it was selected as lead Nb for this study on CRIg expression.

Supplemental References

1. Schmittgen TD, Livak KJ. Analyzing real-time PCR data by the comparative C(T) method. *Nat Protoc.* 2008;3:1101-1108.

2. Schoonooghe S, Kaigorodov V, Zawisza M, et al. Efficient production of human bivalent and trivalent anti-MUC1 Fab-scFv antibodies in Pichia pastoris. *BMC Biotechnol.* 2009;9:70.

3. De Groeve K, Deschacht N, De Koninck C, et al. Nanobodies as Tools for In Vivo Imaging of Specific Immune Cell Types. *J Nucl Med.* 2010;51:782-789.

4. Conrath KE, Lauwereys M, Galleni M, et al. Beta-lactamase inhibitors derived from single-domain antibody fragments elicited in the Camelidae. *Antimicrob Agents Chemother.* 2001;45:2807-2812.

5. Vaneycken I, Govaert J, Vincke C, et al. In vitro analysis and in vivo tumor targeting of a humanized, grafted nanobody in mice using pinhole SPECT/micro-CT. *J Nucl Med.* 2010;51:1099-1106.

6. Cortez-Retamozo V, Lahoutte T, Caveliers V, et al. 99mTc-Labeled Nanobodies: A New Type of Targeted Probes for Imaging Antigen Expression *Curr Radiopharm.* 2008;1:37-41.

7. Put S, Schoonooghe S, Devoogdt N, et al. SPECT imaging of joint inflammation with Nanobodies targeting the macrophage mannose receptor in a mouse model for rheumatoid arthritis. *J Nucl Med.* 2013;54:807-814.

Supplemental Table 1. Biochemical properties for nine evaluated anti-CRIg Nbs.

Nbs	Group	Total amount after SEC (mg/L)	K_D (nmol/L)
NbV4m 68	1	3.2	2.40
NbV4m109	1	6.0	15.4
NbV4m117	1	3.0	19.1
NbV4m120	1	5.4	26.4
NbV4m124	1	11.6	3.70
NbV4m145	1	10.2	32.3
NbV4m 17	2	7.3	1.50
NbV4m 62	2	19.6	1.30
NbV4m119	2	5.0	0.90
NbBCII10	Control	5.0	ND

The Nbs were grouped according to the protein sequence similarity of the complementarity determining region 3. The total yield of purification from bacterial production cultures and the affinities (K_D) from SPR studies are also shown. ND: not detectable. SEC: Size-exclusion chromatography.

Supplemental Table 2. Comparison of in vivo liver-targeting potential in naïve mice among selected ^{99m}Tc-labeled anti-mCRIg Nbs at 1.5 h post injection.

Radiotracer	Liver	L/ B	L/M
NbV4m68	20.2±0.4*	13.2±0.5*	65.5±2.5*
NbV4m62	12.6±1.1*	24.5±4.5*	60.5±13.5*
NbV4m119	23.6±0.1*	28.4±3.2*	116.3±17.5*
NbBCII10	0.6±0.6	1.2±0.1	4.7±1.5

Mean-SD values (n=3) are given for parameters obtained after γ-well counting: liver (%IA/g), liver-to-blood ratio (L/B), liver-to-muscle ratio (L/M). *P<0.05 versus NbBcII10.

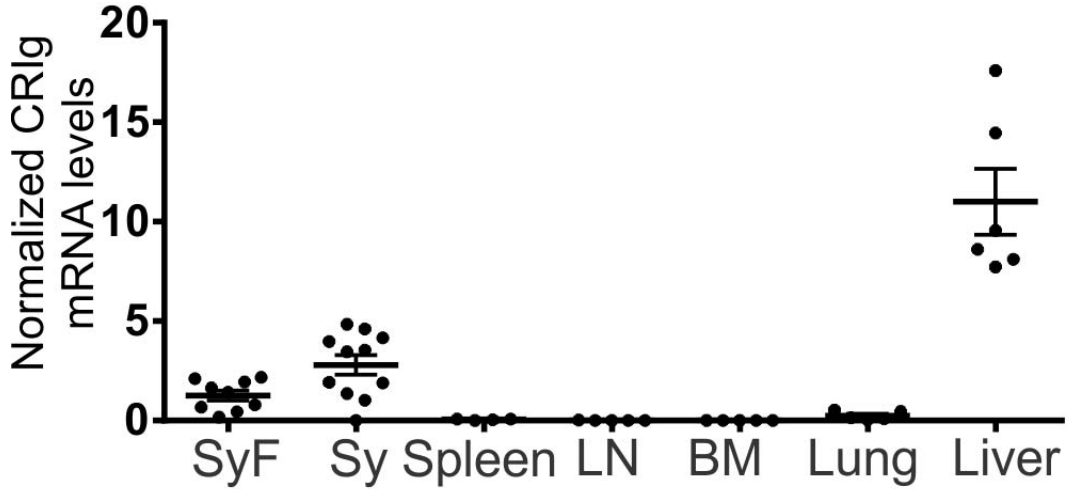

Supplemental figure 1: CRIg mRNA is primarily expressed in the liver and arthritic joints. qPCR on cDNA made from RNA extracted from synovial fluid, synovial tissue, spleen, lymph nodes (LN), bone marrow (BM), lung and liver. Depicted CRIg mRNA levels from CIA mice are normalized against GAPD RNA (n=5 means ± SEM.).

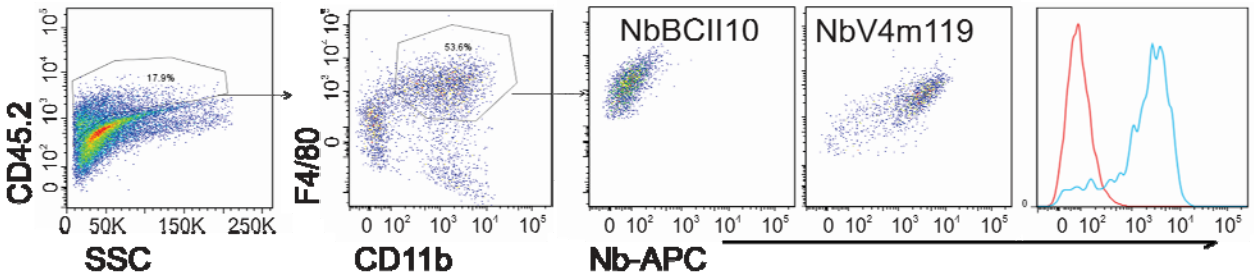

Supplemental Figure 2: Anti-CRIg NbV4m119 specifically targets liver cells in naive C57Bl/6J wild type (WT) but not in CRIg$^{-/-}$ mice. NbV4m119 bind to *ex-vivo* isolated liver macrophages in naive C57Bl/6J wild type (WT) mice. Flow cytometry dot plots are gated on whole leukocytes (CD45.2 positive population). Histogram plots are gated on CD11b^{intermediate}-F4/80^{high} Kupffer cells. Anti-CRIg NbV4m119 specifically targets liver in naive C57Bl/6J wild type (WT) mice but not in CRIg$^{-/-}$ mice.

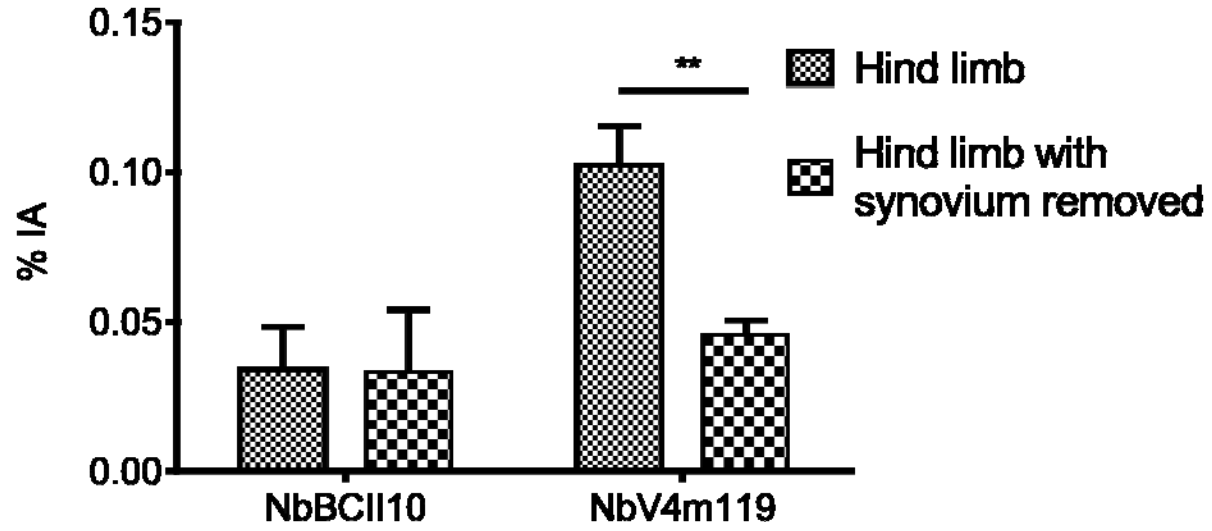

Supplemental Figure 3: Nbs target macrophage-like cells in synovium. Dissection of hind limbs of CIA mice challenged with radiolabeled Nbs. Uptake of ^{99m}Tc-NbV4m119 and ^{99m}Tc-NbBcII10 was compared in hind limbs with intact synovium or with the synovium removed (n=3, mean ± SD, **: P<0.01 versus ^{99m}Tc-NbBcII10).

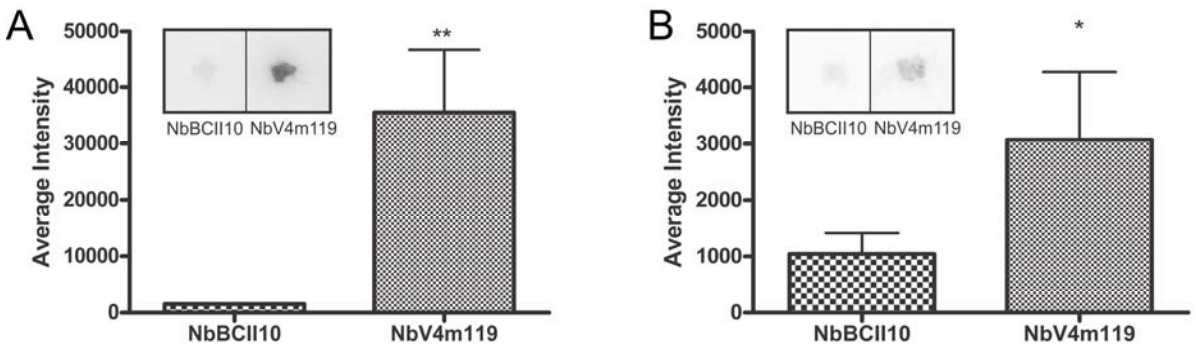

Supplemental Figure 4: ^{99m}Tc-NbV4m119 and ^{99m}Tc-NbBCII10 uptake in knee synovium (A) and ankle synovium (B) of CIA mice were measured by phosphoimaging. The insets show an actual radiograph of the tissue, left: NbBCII10; right: NbV4m119 (n=3, mean ± SD, **: P<0.01 *: *P*<0.05, versus ^{99m}Tc-NbBcII10).

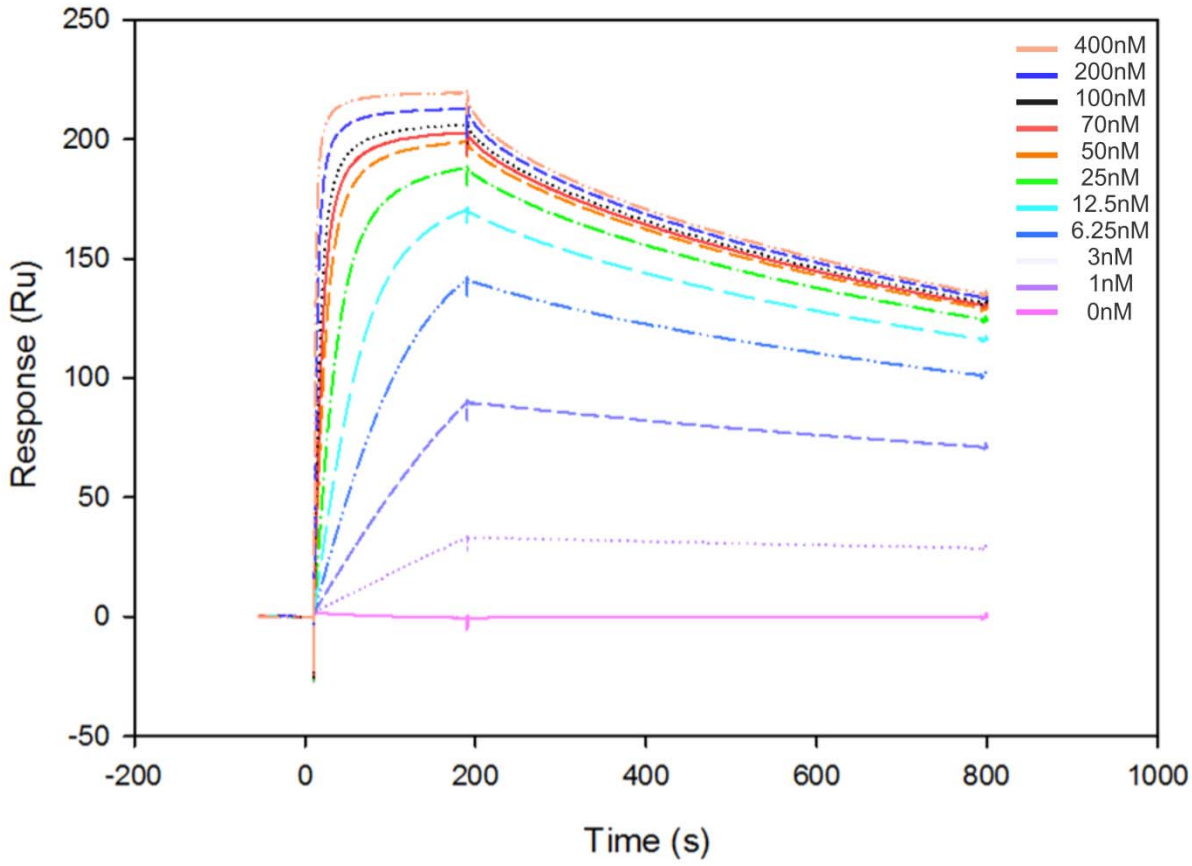

Supplemental Figure 5: Surface plasmon resonance analysis. Representative sensogram of NbV4m119 in a concentration dilution series of 400nM, 200nM, 100nM, 70nM, 50nM, 25nM, 12.5nM, 6.25nM, 3nM, 1nM and 0nM binding to mouse CRIg recombinant protein.

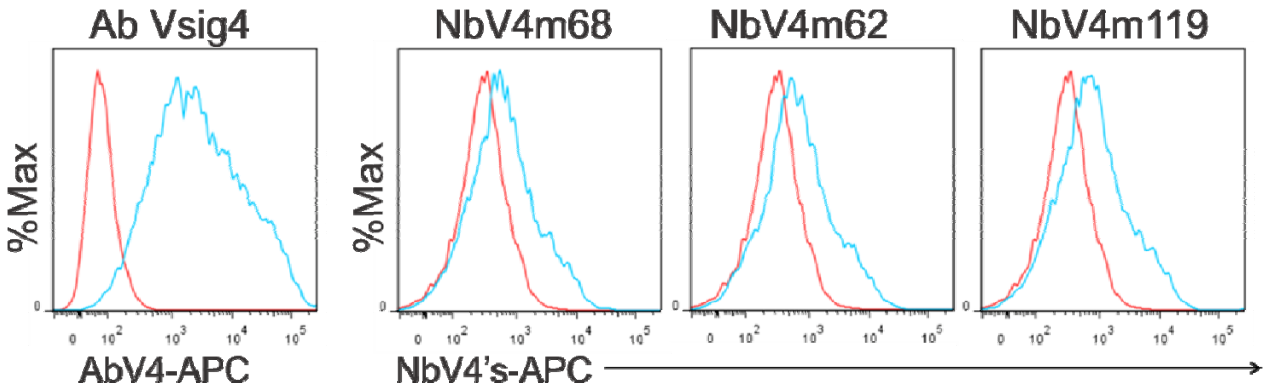

Supplemental Figure 6: Anti-CRIg Nanobodies bind to CRIg transfected cells. Flow cytometry histogram plots of Alexafluor647-labeled anti-CRIg Nbs (blue line) staining CRIg-transfected CHO cells are shown in conjunction with a non-targeting Alexafluor647-labeled NbBCII10 control Nb (red line). Alexa fluor647-labeled CRIg monoclonal antibody (blue line) was used as a positive control in conjunction with an isotype control Ab (red line).

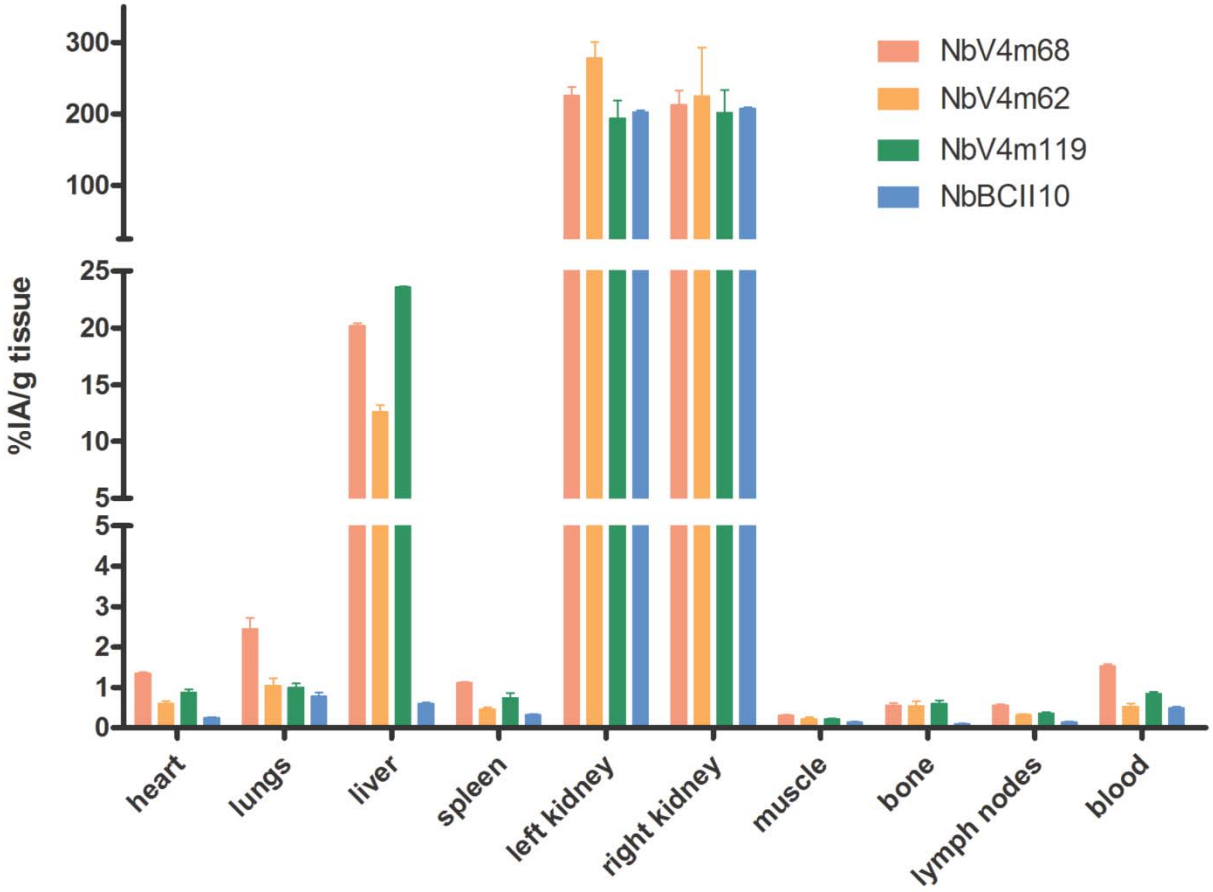

Supplemental Figure 7: ^{99m}Tc-anti-CRIg Nanobody targets CRIg in the liver of naïve C57Bl/6J wild type mice. ^{99m} Tc-NbV4m68, ^{99m} Tc-NbV4m62, ^{99m} Tc-NbV4m119 or ^{99m} Tc-NbBCII10 was injected in C57Bl/6J WT mice (mean of 3 mice ± SEM). Radioactive content of each organ was measured in a γ-counter and expressed as percentage of injected activity per gram tissue (%IA/g), ***: $P<0.001$, **: $P<0.005$, *: $P<0.05$ versus ^{99m}Tc-NbBCII10.

Supplemental Video 1: Full 3D reconstruction of whole body SPECT/CT images visualizing ^{99m}Tc-NbV4m119 biodistribution in CIA mice. CIA mice were injected with ^{99m}Tc-NbV4m119 i.v. and were scanned 3 hours p.i. Bone structures, visualized by CT are gray scale encoded. Radioactive signals obtained by SPECT are NIH + white color encoded: from black (no signal) to violet, blue, green, yellow, orange, red (high intensity signal) and white (saturated signal). The clinical scores (also shown in Figure 2B) for the animal were: front right paw = 3, front left paw = 0, right hind paw = 3, left hind paw = 4. ^{99m}Tc-NbV4m119 accumulated in paws with clinical scores. The Nanobody was also observed in the liver (specific binding to CRIg^{+} Kupffer cells) and in the kidneys and bladder (associated with tracer clearance from the body). The reconstruction of a representative mouse is shown.

Supplemental Video 2: Full 3D reconstruction of whole body SPECT/CT images visualizing ^{99m}Tc-NbBCII10 biodistribution in CIA mice. CIA mice were injected with ^{99m}Tc-NbBCII10 i.v. and were scanned 3 hours p.i. Bone structures, visualized by CT are gray scale encoded. Radioactive signals obtained by SPECT are NIH + white color encoded: from black (no signal) to violet, blue, green, yellow, orange, red (high intensity signal) and white (saturated signal). The clinical scores (also shown in Figure 2C) for the animal were: front right paw = 3, front left paw = 0, right hind paw = 4, left hind paw = 0. No specific ^{99m}Tc-NbBCII10 accumulation was observed in the joints. Only the kidneys and bladder demonstrated a high Nanobody signal associated with tracer clearance from the body. The reconstruction of a representative mouse is shown.

Supplemental Video 3: Full 3D reconstruction of whole body SPECT/CT images visualizing ^{99m}Tc-NbV4m119 accumulation in an inflamed knee with a low clinical score associated

with the corresponding paw. Uptake of the CRIg-specific Nanobody in different types of joints reveals additional variability that goes beyond the limitations of the clinical scoring system. CIA mice were injected with ^{99m}Tc-NbV4m119 i.v. and were scanned 3 hours p.i. Bone structures, visualized by CT are gray scale encoded. Radioactive signals obtained by SPECT are NIH + white color encoded: from black (no signal) to violet, blue, green, yellow, orange, red (high intensity signal) and white (saturated signal). The clinical scores for this mouse were: front right paw = 0, front left paw = 3, right hind paw = 1, left hind paw = 1. In this animal the inflammation present in the knee was imaged with the ^{99m}Tc-NbV4m119 although the limb was only graded 1 in the clinical scoring system, because the scoring does not take the status of the knee into consideration. However, in the front left paw the high ^{99m}Tc-NbV4m119 signal did correspond to the clinical score 3 awarded to this limb. Also of note is the high Nanobody signal in the elbow of the front left limb. The Nanobody was also observed in the liver (specific binding to CRIg$^+$ Kupffer cells) and in the kidneys and bladder (associated with tracer clearance from the body). The reconstruction of a representative mouse is shown.

Supplemental Video 4: Full 3D reconstruction of whole body SPECT/CT images of ^{99m}Tc-V4m119 accumulation in joints of CIA mice before onset of arthritis symptoms. Pre-symptomatic CIA mice (Figure 5C) without any visible symptoms (clinical scores all 0) of arthritis were injected with ^{99m}Tc-NbV4m119 i.v. at d23 post immunization. The mice were scanned 3 hours p.i. and bone structures, visualized by CT are gray scale encoded. Radioactive signals obtained by SPECT are NIH + white color encoded: from black (no signal) to violet, blue, green, yellow, orange, red (high intensity signal) and white (saturated signal). In this particular animal ^{99m}Tc-NbV4m119 uptake was observed in the right knee. The right hind paw developed

arthritis at a later stage and was graded with a clinical score of 1 by d26 and score 2 by d31. The Nanobody was also observed in the liver (specific binding to $CRIg^+$ Kupffer cells) and in the kidneys and bladder (associated with tracer clearance from the body). The reconstruction of a representative mouse is shown.